

On Plant Modeling for the PIM Digital Redesign of a Power System Stabilizer

G. SHABIB

Department of Electrical Engineering
South Valley University
Aswan Higher Institute of Energy, Aswan
EGYPT
gabershabib@yahoo.com

Abstract: - This paper is concerned with the plant modeling for the digital redesign of a continuous-time power system stabilizer PSS for the single machine power system using the so-called Plant –Input-Mapping PIM method. The traditional approach has been to use the bilinear transform (Tustin’s method), but this gives numerical difficulties with large sampling intervals which are now becoming usual with modern control hardware. The proposed technique guarantees the stability for any sampling rate and takes the closed-loop characteristics into account. The proposed technique is successfully applied to the discretization of a continuous time PSS for single-machine power system. For comparison studies the proposed technique is compared with continuous-time PSS and Tustin’s PSS. The simulation results show that the proposed digital redesign technique reflects the frequency and dynamic responses of the system more accurately as the continuous-time PSS. Also, they show that Tustin’s method falls when sampling interval becomes larger while the proposed PIM method guarantees stability even with relatively slow sampling rates.

Key-Words: - Digital redesign, Discretization, Dynamic stability, Power systems, Sampled-data system.

1 Introduction

The increasing complexity of power system requires the use of digital devices. They are widely spread and play an essential task in the operation of power systems. Several kinds of digital controlled devices are used in practical in power system now days, such as digital AVR, digital PID controller and digital PSS.

The use of digitally controlled systems offers a wide range of possibilities such as:

1. Changing a few parameters or implementing a complete new strategy in most cases is just a matter of recompiling a software program model, which on contrary to analog control system that changing components.
2. Relatively low cost and high computational speeds can be provided with almost any size process.
3. The ability to interface readily with other computer systems and integration with remote

systems.

4. Easier to implement complicated algorithms.
5. Greater range of control algorithms can be used e.g. adaptive control techniques.

Digital redesign can be defined as the process of converting a previously well-designed continuous time controller to a suitable discrete-time controller suitable for digital implementation, such that the states of the continuous-time and that of the discrete-time closed loop systems can match each other. The common conventional methods used to discretize analog controllers are the sample and hold equivalence and bilinear transformation or Tustin's method [1]. These two methods produce satisfactory results provided that the sampling rate should be sufficiently fast. However, they are open loop based, i.e. there is no consideration of closed loop stability and performance in the discretization process. Furthermore, with such design methods and processors, full potential of control algorithms is not utilized. It is imperative, therefore, to develop a high performance digital control law that can be implemented on a slower and low cost processor currently available.

Some other approaches to the solution were presented in [2, 3]. Ref. [4] presents the asymptotical stability of the digital controls of power systems with special emphasis on the digital power system stabilizer; this paper treats power system with digital controller as nonlinear hybrid dynamical systems. In [5] an optimal digital redesign of conventional power system stabilizers for single machine power system are presented; it is based on an optimal matching of the continuous-time closed loop step responses of both analog and discretized systems. Ref. [6] presents a model-matching robustness design procedure based

on H_∞ optimization theory; the method uses a control law designed for the nominal operating condition and tunes the nominal control law to enhance the robustness with respect to the off-nominal operating conditions. Other optimization based discretization has been found in [7, 8]. However, these algorithms are either too complicated or state-space based.

The plant-Input-Mapping (PIM) method [9,10,11,12] is a method of discretization that can guarantee, in theory, the stability for virtually any sampling rates (non-pathological sampling rates) and that has good performances even for large sampling intervals. Unlike the popular conventional method of discretization, the PIM method takes the closed-loop characteristics into account. This paper uses the PIM method to design a digital PSS for the power system. The PSS is widely used in power system to generate supplementary control signal for the excitation system in order to damp the low frequency oscillations [13]. Using the proposed PIM approach, the stability of the digital control system is guaranteed for any non-pathological sampling periods, i.e. those sampling periods which do not hide unstable natural frequencies, if any, of the plant. It should be emphasized that no other existing digital redesign method can guarantee the stability if the sampling period is not sufficiently small.

This paper is organized as follows. In section 2, for SISO linear time invariant system, a design procedure for the three controller blocks PIM digital redesign method is considered. Section 3 consists of three subsections which are drive a power system model; explain the power system stabilizer PSS model used in the study and finally the application of the PIM method to a single-machine power system. The conclusions are given in section 4.

2 The Three Controller Blocks PIM Digital Redesign Method

Consider the SISO system shown in Fig.(1), which consists of plant with a strictly proper transfer function $G_c(s)$ and three analog controllers with rational, proper transfer functions $R_c(s)$, $C_c(s)$ and $F_c(s)$.

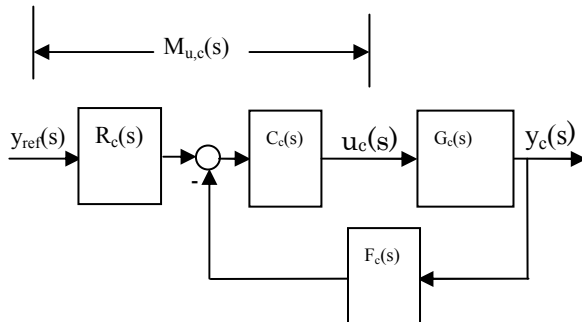


Fig.1 Three controllers of linear and time-invariant analog control system

The Transfer function $M_{u,c}(s)$ is defined as the transfer function from the reference input $y_{ref}(s) = \mathcal{L}\{y_{ref}(t)\}$ to the plant input $u_c(s) = \mathcal{L}\{u_c(t)\}$ of the analog system, where \mathcal{L} denotes Laplace transform. For simplicity, this is called the continuous-time plant-input transfer function CT-PITF.

$$u_c(s) = y_{ref}(s)C_c(s)R_c(s) - F_c(s)C_c(s)G_c(s)u_c(s) \quad (1)$$

By rearranging Eq. (1), it can be written in the following form

$$M_{u,c}(s) = \frac{u_c(s)}{y_{ref}(s)} = \frac{R_c(s)C_c(s)}{1 + F_c(s)C_c(s)G_c(s)} \quad (2)$$

The overall transfer function $T_c(s)$ is defined

$$T_c(s) = G_c(s)M_{u,c}(s) \quad (3)$$

since $T_c(s)$ is stable by assumption, $M_{u,c}(s)$ is stable. Furthermore, a condition required for closed-loop stability can be related to the condition on the PITF in the following manner [10].

The transfer function of the plant $G_c(s)$ is given by

$$G_c(s) = \frac{n_c(s)}{d_c(s)} \quad (4)$$

where $\partial [d_c(s) = \bar{n} \geq \partial [n_c(s)]]$ and ∂ denotes the degree of its argument variable. It is assumed that the polynomials $n_c(s)$ and $d_c(s)$ are coprime.

This transfer function can be expressed in the coprime fractional form as [14].

$$G_c(s) = \frac{N_c(s)}{D_c(s)} \quad (5)$$

where

$$N_c(s) = n_c(s)\lambda^{-1}(s) \in M^\infty,$$

$$D_c(s) = d_c(s)\lambda^{-1}(s) \in M^\infty \quad (6)$$

$\lambda(s)$ is an arbitrary but stable polynomial $[\partial \lambda(s) \leq \bar{n}]$. The symbol M^∞ denotes the space of real, rational, and stable transfer function [14].

The CT-PITF $M_{u,c}(s) \in M^\infty$ if and only if there exist a $W(s) \in M^\infty$ such that

$$H_{u,c}(s) = D_c(s)W(s) \quad (7)$$

Eq. (7) implies that, since $W(s) = D_c^{-1}(s)M_{u,c}(s)$, all poles of the plant that need to be controlled, must appear as the zeros of the CT-PITF and disappear from $W(s)$ for closed loop stability [15].

The plant transfer function $G_c(s)$ is now discretized using the step invariant-model SIM, which is a combination of the zero-order-hold (ZOH), the plant and the sampler, synchronized with a non-pathological sampling period T as shown in Fig.(2).

The transfer function of the SIM is given by [10]

$$G_T(\epsilon, T) = \frac{\epsilon}{T\epsilon + 1} D\left(\frac{G_c(s)}{S}\right) \quad (8)$$

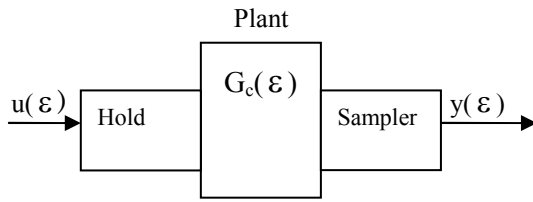


Fig. 2 Step invariant model SIM of the plant

The ϵ in the numerator is always cancelled out by the D transform of the S in the denominator. Since the D transform of $G_c(s)$ usually contains $T\epsilon + 1$ in its numerator, the $T\epsilon + 1$ term in the denominator is cancelled out, giving the DT model whose order is the same as CT system. The discretize SIM plant model has no unstable pole-zero cancellation for any nonpathological sampling interval.

The order of system after discretization is $\partial [D_T(\epsilon, T)] = n \leq \bar{n}$. As in the case, introducing an n^{th} degree, arbitrary but stable polynomial $\lambda(\epsilon, T)$, the SIM of the plant can be written in the following coprime fractional form:

$$G_T(\epsilon, T) = N_T(\epsilon, T)D_T^{-1}(\epsilon, T) \tag{9}$$

where

$$N_T(\epsilon, T) \in M^\infty, D_T(\epsilon, T) \in M^\infty$$

The overall transfer function is given by

$$T_T(\epsilon, T) = G_T(\epsilon, T)M_{u,T}(\epsilon, T) \tag{10}$$

where $M_{u,T}(\epsilon, T)$ is the DT-PITF which used later in designing the PIM model and $M_{u,T}(\epsilon, T) \in M^\infty$. For digital controller that will be replaced analog controller the zeros of the DT-PITF should be mapped in the same manner as the poles of the plant. This can be achieved by using any of the matched pole zero MPZ discretization schemes [10]. In this case $M_{u,c}(\epsilon, T)$ denotes a MPZ model of $M_{u,c}(s)$, and written as

$$M_{u,T}(\epsilon, T) = \frac{D_T(\epsilon, T)m(\epsilon, T)}{d_M(\epsilon, T)}$$

(11)

where $D_T(\epsilon, T)$ is the denominator transfer function of the SIM plant model. Since T is nonpathological, the coprimeness of $N_T(\epsilon, T)$ and $D_T(\epsilon, T)$ are preserved in the DT plant model, and there are exist transfer functions $\alpha(\epsilon, T) \in M^\infty$ and $\beta(\epsilon, T) \in M^\infty$ such that the following Diophantine equation holds

$$\alpha(\epsilon, T)D_T(\epsilon, T) + \beta(\epsilon, T)N_T(\epsilon, T) = d_M(\epsilon, T) \tag{12}$$

Eq. (12) can be solved to find the unknown terms $\alpha(\epsilon, T)$ and $\beta(\epsilon, T)$. Fig. (3) shows the block diagram of the PIM model.

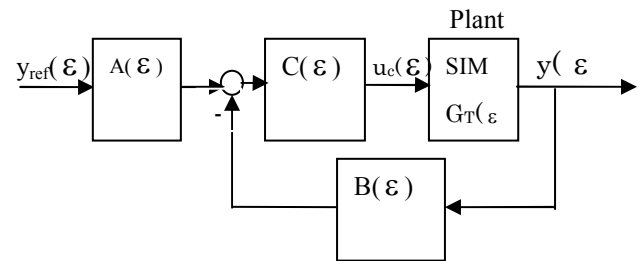


Fig. 3 PIM design method for a plant

The three controller blocks $A(\epsilon)$, $C(\epsilon)$ and $B(\epsilon)$ are polynomials in ϵ and can be selected as

$$A(\epsilon) = \frac{m(\epsilon, T)}{\lambda(\epsilon, T)}$$

$$C(\epsilon) = \frac{\lambda(\epsilon, T)}{\alpha(\epsilon, T)}$$

$$B(\epsilon) = \frac{\beta(\epsilon, T)}{\lambda(\epsilon, T)}$$

(13)

where $m(\epsilon, T)$ is a stable polynomial and calculated from Eq. (11) by dividing the numerator of $M_{u,T}(\epsilon, T)$ by denominator of SIM of the plant. For stable plant the DT-PITF must satisfy the following equation

$$M_{u,T}(\varepsilon, T) = \frac{A(\varepsilon, T)C(\varepsilon, T)}{1 + (\varepsilon, T)G_T(\varepsilon, T)B(\varepsilon, T)}$$

(14)

The PIM design guarantees the internal stability for any nonpathological sampling interval and that the performance of the resulting control system approaches that of the analog control system as $T \rightarrow 0$.

3 Applications to a Single-Machine Power System

3.1 Power System Model

The power system considered in this study is the fourth order linearized one-machine and infinite-bus system described in [16]. Fig.4 shows a block diagram of transfer functions describing the different subsystems of the one machine infinite bus power system, where the blocks are

1- Excitation system

$$\frac{K_e}{1 + ST_e}$$

(15)

where K_e and T_e are voltage regulator gain and time constant respectively.

2- Field flux decay

$$\frac{K_3}{1 + SK_3T'_{d0}}$$

(16)

where T'_{d0} is the d-axis transient open circuit time constant.

3-Machine mechanical dynamics loop

$$\frac{1}{2HS + D}$$

(17)

Where H is the inertia constant.

K_1, \dots, K_6 are the constant of linearized model of synchronous machine.

From the block diagram shown in Fig.(4), and using Eqs. (15)-(17) the following fourth order linearized one machine infinite bus system can be derived as described in [16] and is given in state variable form as follows:

$$\begin{aligned} \dot{x} &= Ax + Bu \\ y &= Cx + Du \end{aligned}$$

(18)

where

$$A = \begin{bmatrix} -\frac{D}{2H} & -\frac{K_1}{2H} & -\frac{K_2}{2H} & 0 \\ \omega_B & 0 & 0 & 0 \\ 0 & -\frac{K_4}{T'_{d0}} & -\frac{1}{T'_{d0}K_3} & \frac{1}{T'_{d0}} \\ 0 & -\frac{K_eK_5}{T_e} & -\frac{K_eK_6}{T_e} & \frac{1}{T_e} \end{bmatrix}$$

$$B^T = \begin{bmatrix} \frac{1}{2H} & 0 & 0 & 0 \end{bmatrix}, \quad C^T = \begin{bmatrix} 1 & 0 & 0 & 0 \end{bmatrix}$$

The state variables comprise the generator are speed deviation $\Delta\omega$, rotor angle deviation $\Delta\delta$, transient internal voltage deviation $\Delta E'_q$, and field voltage deviation ΔE_{fd} , respectively. The deviation of the angular velocity $\Delta\omega$ is assumed to be measured as the output of the system. The constants of the generation system and connected power system used for study are

Generator parameters:

$$H=4.63, D=4.4, T'_{d0}=7.67, \omega_B=377.0, X_d=0.973$$

$$\text{pu}, x'_d=0.19 \text{ pu}, X_q=0.55 \text{ pu}$$

Exciter parameters:

$$K_e=50.0, T_e=0.05.$$

$$\text{The } K\text{'s: } K_1=0.5758, K_2=0.9738, K_3=0.6584, K_4=0.5266, K_5=-0.0494, K_6=0.8450.$$

PSS parameters:

$K=20.0, T_1=10, T_2=.15, T_3=.05, T_4=0.05, T_5=0.15$

Transmission line:

$R_e=0.0, X_e=0.997$ pu.

Operating point:

$Q_{e0}=0.015$ pu, $V_{t0}=1.05$ pu, $P_{e0}=0.75$ pu.

The damping coefficient D is included in the swing equation. The eigenvalues of the matrix A should lie in LHP in the S-plane for the system to be stable. It is to be noted that the elements of matrix A are depended on the operating condition. The values of K_1, \dots, K_6 in the matrix A are to be selected according to the operating conditions of the generation system and connected power system [17]. Details of these constants are given in appendix I.

Using the data given above, the transfer function of the power system $G_c(s)$ given by Fig. (4) and the state space equations given by Eq. (18) can be calculated using the MATLAB function SS2F in the signal processing toolbox and are given by:

$$G_c(s) = \frac{0.108s^3 + 2.181s^2 + 12.18s + 3.183 \times 10^{-12}}{s^4 + 20.63s^3 + 145s^2 + 519.2s + 2843} \quad (19)$$

The power system contains double complex poles at $S = -10.22 \pm j3.516$ and at $S = -0.0938 \pm j4.9329$ and contains a zeros at $S = -10.0979 \pm j3.2923$ and at

$S=0.0$

3.2 Continuous Time Power System Stabilizer PSS Model

The continuous time PSS type is widely used in the power system to improve the damping oscillations of the power system; sometime it is called the damping controller. Because the power system is very oscillatory, the objective of the PSS is to enhance the damping force and necessarily to improve the dynamical stability of the power system.

The PSS is considered as comprising two cascade connected blocks, commonly lead-lag structure [18]. The transfer function of a continuous-time, lead-lag type, power system stabilizer is given by

$$PSS(s) = \left(\frac{KS}{1+ST_1} \right) \left(\frac{1+ST_3}{1+ST_2} \right) \left(\frac{1+ST_5}{1+ST_4} \right) \quad (20)$$

The gains K is chosen by trial and error method and the wash out time constant T_1 is chosen in between 0 to 20. The wash-out stage is used to prevent a steady

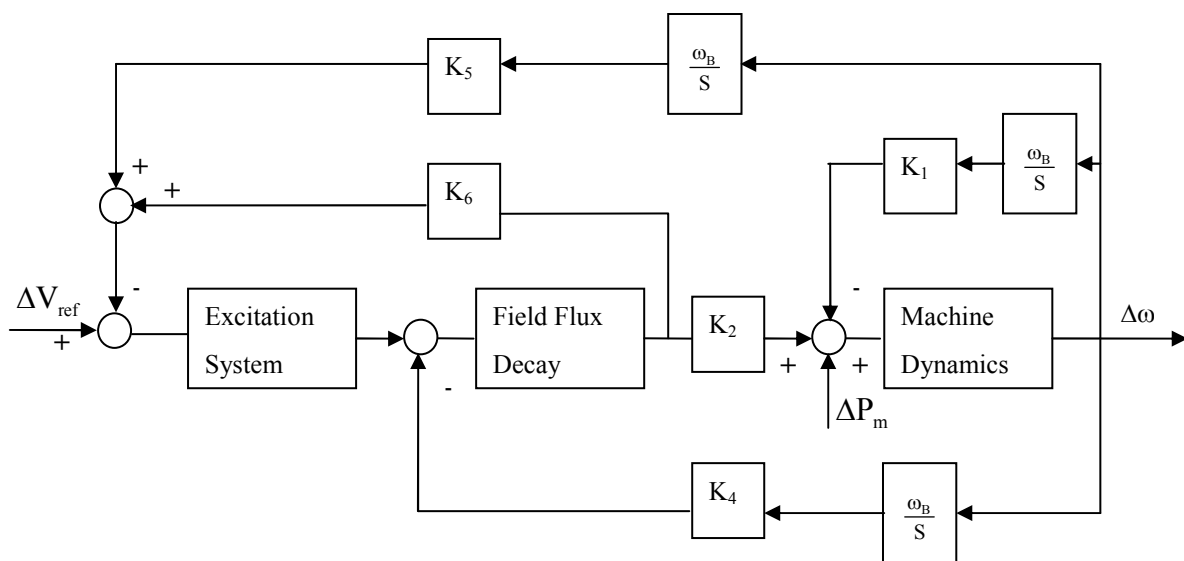


Fig. 4 Block diagram of one machine infinite bus system

-state voltage shift; T_2, T_3, T_4 and T_5 are time constants of the two phase-lead stages.

Fig. 5 shows the block diagram of the PSS. The parameters of PSS is tuned by using trail and error method, so as to achieve the desired damping ratio of the electromechanical mode and compensate for the phase shift between the control signal and the resulting electrical power deviation.

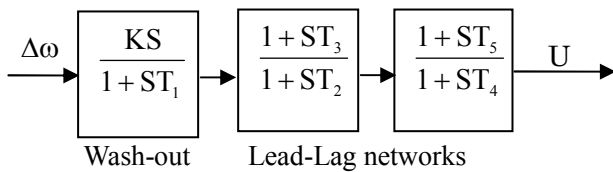


Fig. 5 Block diagram of the PSS

Utilizing the data of the PSS given, the transfer function of the PSS described by Eq.(20) can be calculated as follows

$$PSS(s) = \frac{1.5S^3 + 40S^2 + 200S}{0.075S^3 + 2.007S^2 + 10.2S + 1} \tag{21}$$

The PSS has three poles at $S=-20, S=-6.667$ and $S=-0.1$, respectively, and has a three zeros at $S=0.0, S=-20$ and at $S=-6.667$.

For steady-state stability study and power system stabilizer design, ΔP_m and ΔV_{ref} are assumed to be equal zero. Fig. (4) can therefore redrawn as in Fig. (6), where $G_c(s)$ is the transfer function of the block diagram given by Fig. (4), a block with transfer function -1 is introduced in order to form a negative feedback system. The PSS is now acting as a dynamic feedback controller for SISO control system [17].

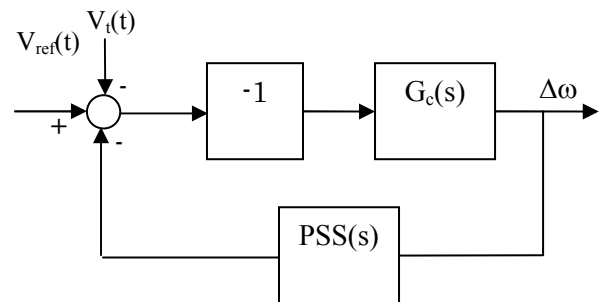


Fig. 6 Single-Input Single-Output feedback system

3.3 Application of PIM Digital Redesign Method to Power System Model

To apply the design technique presented in section 2, the transfer function $G_c(s)$ for the power system given by Eq. (19) and the transfer function $PSS(s)$ for the power system stabilizer given by Eq. (21) are used in the design procedure with the blocks $R_c(s)$ and $C_c(s)$ equal to 1.

Simulations responses of the power system based on the linear model given by Eq. (18) are presented. The power system is subject to a step change in the mechanical torque denoted by ΔP_m . The signal to be controlled is the rotor speed denoted by $\Delta \omega$. The analog PSS is placed on the block $F_c(s)$ of Fig. (1) of the three block controllers PIM digital redesign method. For comparison, results of the analog PSS and the digital PSS obtained by the bilinear transformation (Tustin's method) are investigated.

The CT-PITF is found to be

$$M_{u,c}(s) = \frac{(S + 20)(S + 6.667)(S + 0.1)(S^2 + 20.44S + 116.8)(S^2 + 0.187S + 24.34)}{(S + 20)(S + 6.667)(S + 0.1)(S^2 + 20.51S + 117.8)(S^2 + 2.273S + 23.93)}$$

It is clear that all power system poles and PSS poles are appear in the numerator of the CT-PITF (Eq. 7).

The MPZ model of the ZOH type with its DC gain adjusted is used for discretizing the CT-PITF and is

given as

$$M_{u,T}(\varepsilon) = \frac{0.91895(\varepsilon + 5.167)(\varepsilon + 9.976)(\varepsilon + 0.0996)(\varepsilon^2 + 14.4\varepsilon + 54.15)(\varepsilon^2 + 2.0944\varepsilon + 23.85)}{(\varepsilon + 9.976)(\varepsilon + 5.167)(\varepsilon + 0.1005)(\varepsilon^2 + 14.44\varepsilon + 54.47)(\varepsilon^2 + 3.807\varepsilon + 21.6)}$$

The SIM model of the power system is given by

$$G_T(\varepsilon) = \frac{0.10351\varepsilon(\varepsilon^2 + 14.24\varepsilon + 52.74)}{(\varepsilon^2 + 14.4\varepsilon + 54.15)(\varepsilon^2 + 2.094\varepsilon + 23.85)}$$

The sampling interval selected for digital control is 0.08sec, (any sampling interval $T > 0$ is nonpathological) which is reasonable compared with the dynamic of the system.

The polynomial $\lambda(\varepsilon, T)$ is selected as

$$\lambda(\varepsilon, T) = (\varepsilon + 1/2T)^2$$

The polynomial $m(\varepsilon, T)$ is obtained from the numerator of $M_{u,T}(\varepsilon, T)$ which is

$$m(\varepsilon, T) = 0.9189\varepsilon^3 + 14.0072\varepsilon^2 + 48.7547\varepsilon + 4.718$$

It is clear that the numerator of $M_{u,T}(\varepsilon, T)$ includes the poles of the SIM of the power system and the polynomial $m(\varepsilon, T)$.

Using the numerator and denominator of the SIM of power system the eliminant matrix can be constructed as follows

$$E = \begin{bmatrix} 1.0 & 0 & 0 & 0 & 0 & 0 & 0 & 0 \\ 16.5 & 1.0 & 0 & 0 & 0.1 & 0 & 0 & 0 \\ 108.1 & 16.5 & 1.0 & 0 & 1.5 & 0.1 & 0 & 0 \\ 456.7 & 108.1 & 16.5 & 1.0 & 5.5 & 1.5 & 0.1 & 0 \\ 1291.5 & 456.7 & 108.1 & 16.5 & 0 & 5.5 & 1.5 & 0.1 \\ 0 & 1291.5 & 456.7 & 108.1 & 0 & 0 & 5.5 & 1.5 \\ 0 & 0 & 1291.5 & 456.7 & 0 & 0 & 0 & 5.5 \\ 0 & 0 & 0 & 1291.5 & 0 & 0 & 0 & 0 \end{bmatrix}$$

Solving Eq. (12) with the aid of the eliminant matrix given above, the polynomial $\alpha(\varepsilon, T)$ and $\beta(\varepsilon, T)$ are obtained and equal to

$$\alpha(\varepsilon, T) = \varepsilon^3 + 15.1081\varepsilon^2 + 52.8022\varepsilon + 4.718$$

$$\beta(\varepsilon, T) = 18.238\varepsilon^3 + 243.562\varepsilon^2 + 629.3123\varepsilon - 956.442$$

For ease of relating discrete-time systems to continuous-time counterparts, the following operator is used

$$\varepsilon = \frac{z - 1}{T}$$

where T is the sampling interval and z the usual zee operator. The three controller blocks $A(z)$, $C(z)$ and $B(z)$ are calculated using the results obtained above and are given below;

$$A(z) = \frac{m(z, T)}{\lambda(z, T)} = \frac{0.919z^3 - 1.636z^2 + 0.8277z - 0.108}{z^3 - 1.5z^2 + 0.75z - 0.125}$$

$$B(z) = \frac{\lambda(z, T)}{\alpha(z, T)} = \frac{z^3 - 1.5z^2 + 0.75z - 0.125}{z^3 - 1.791z^2 + 0.9204z - 0.1269}$$

$$C(z) = \frac{\beta(z, T)}{\lambda(z, T)} = \frac{18.17z^3 - 35.11z^2 + 19.71z - 3268}{z^3 - 1.5z^2 + 0.75z - 0.125}$$

Referring to Figs. (7)- (9) it is clear that, at high sampling rates the rotor speed deviation responses $\Delta\omega$ of all PSS's are matches, The performances of Tustin's and the PIM PSS's are almost the same as that of the analog PSS at the control rate 12.5Hz. Since the PIM and the Tustin's PSS realize the same PITF, their plant inputs and behaviors are always identical to each other in ideal simulations. At 5Hz control rate, the Tustin's response produces a larger overshoot than the analog case, while the PIM designs yield the response that is identical to the analog one. At 2.12 Hz control rate, Tustin's response oscillates to such an extent that it is not acceptable. Although the PIM PSS yields transient responses that is different from analog case, their performance is very good. The settling time is in

fact faster than the analog PSS, which is not intended. As a summary, almost identical characteristics are obtained for the PIM method and the continuous-time model which confirm the accuracy of the proposed PIM method in low and high sampling rates.

The pole-zero location of the overall transfer function considering sampling interval of 0.08 sec is shown in Table 1 for the case of continuous-time PSS, and Table 2 for the case of PIM PSS.

Table 1 Case of continuous-time PSS

| poles | zeros |
|-----------------|------------------|
| -20.0 | -20.0 |
| -10.22±J3.5491 | -0.0938±J4.9329 |
| -0.0938±J4.9239 | -10.0979±J3.2923 |
| -6.6667 | -6.6667 |
| -0.1009 | -0.100 |

Table 2 Case of PIM PSS

| poles | zeros |
|---------------|-----------------|
| -9.976 | -9.976 |
| -7.24±J1.6194 | -7.22±J1.6098 |
| -1.92±J4.2301 | -1.0665±J4.7626 |
| -5.167 | -0.0992 |
| -0.1005 | -0.000 |

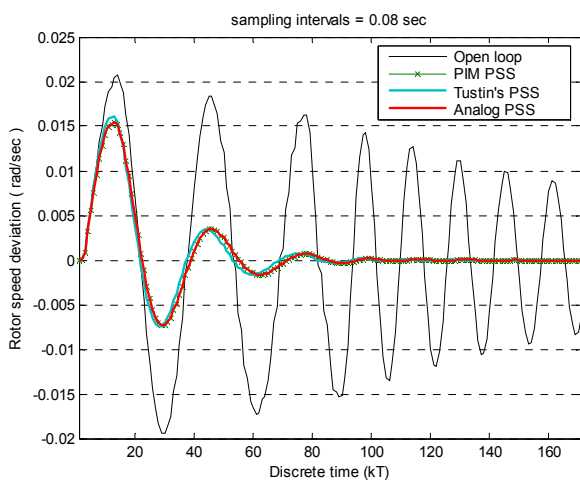


Fig. 7 Dynamic responses to step change in the mechanical torque (sampling interval 0.08 sec)

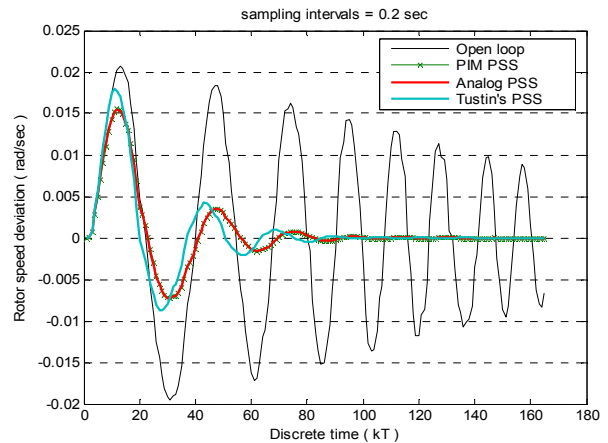


Fig. 8 Dynamic responses to step change in the mechanical torque (sampling interval 0.2 sec)

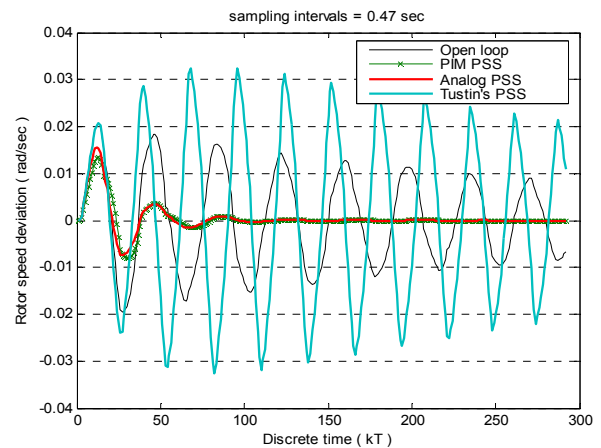


Fig. 9 Dynamic responses to step change in the mechanical torque (sampling interval 0.47 sec)

4 Conclusions

In this paper, a systematic methodology for design of PIM digital redesign scheme was presented, and then we apply it to discretize a continuous-time PSS for single-machine infinite-bus power system. The results observed by simulations showed that states via the proposed PIM digital redesign method match more closely with those of the original continuous-time system. Because digital PIM method are designed based on matching continuous-time ones, it is important to have a

well-designed continuous-time PSS to start with. Tustin's method fall when sampling interval becomes larger while the proposed PIM method guarantee stability even with relatively slow sampling rates which satisfy the hardware requirements.

The proposed method can be extended to be applicable to use nonlinear model for the power system, which will be presented at the next opportunity.

Acknowledgement

The author wish to acknowledge Prof. Hori for his continuous help throughout the progress of this work. The acknowledgment is further extended to the University of Tsukuba, Digital Control Laboratory, 1-1-1 Tennoudai, Ibaraki, 305-8573, Tsukuba, Ibaraki, Japan for the facilities provided.

References

[1] G. F. Franklin, J. D. Powell, and M. Workman, "Digital Control of Dynamic Systems", Addison-Wesley, 1998.

[2] D. Raviv, E.W. Djaja, "Technique for enhancing the performance of discretized controllers", IEEE Control Systems Mag. 19 (3) (1999) 52–57.

[3] Y.N. Rosenwasser, B.P. Lampe, "Parametric transfer functions for sampled-data systems with time-delayed controllers", Proceedings of the IEEE Conference on Decision and Control, San Diego, CA, Vol. 2, December 1997, pp. 1609–1614.

[4] L. Chen, H. Tanaka, K. Katou, and Y. Nakamura, "Stability analysis for digital controls of power systems", Electric Power Systems Research Vol. 55, 2000, pp. 79–86

[5] N. Rafee, T. Chen, O. P. Malik, "A technique for optimal digital redesign of analog controllers", IEEE Transactions on Control Systems Technology, 1996, Vol. 3. Issue 1.

[6] G.N. Taranto, J.H. Chow, H.A. Othman, "Robust redesign of power system damping controllers" IEEE Transactions on Control Systems Technology, 1995, Vol. 3. Issue 3.

[7] T. Chen, B.A. Francis, "H_∞ optimal sampled-data control", IEEE Trans. Automatic Control 36 (4), 1991, pp. 387–397.

[8] J.P. Keller, B.D.O. Anderson, "A new approach to the discretization of continuous-time controllers", IEEE Trans. Automatic Control 37, 1992, pp. 214–223.

[9] A. H. Markazi, N. Hori, K. Kanai, and T. Ieko, "New Discretization of Continuous-Time Control Systems and its Application to the Design of Flight Control System", Proc. 32nd SICE Annual Conf., Kanazawa, Japan, pp. 1199-1203, 1993.

[10] N. Hori, T. Mori, P. N. Nikiforuk, "A new perspective for discrete-time models of a continuous-time systems", IEEE Trans. on Automatic Control, VOL. 37-7, pp 1013-1017, 1992.

[11] T. Okada and N. Hori, "Improved PIM Digital Driver with Dead-Zone Compensation for a Stepping Motor" ICROS-SICE Int. Joint Conf., Fukuoka, Japan, pp. 798-803, August 2009.

[12] R. Takahashi, N. Hori, and W.-X. Sun, "Digital Design of a Current Regulator for Stepping-Motor Drivers Based on Plant-Input-Mapping" Proc. Int. Automatic Control Conf., Taichung, Taiwan, pp. 155-160, November 2007.

[13] E.V. Larsen, D.A. Swann, "Applying power system stabilizers part I, II, III", IEEE Trans-on Power Apparatus and Systems, PAS-100, No.6, pp3017-3041, 1981.

- [14] R.H. Middleton and G. C. Goodwin, "Digital control and Estimation- a Unified Approach", Prentice-Hall, Englewood Cliffs, NJ (1990).
- [15] M. K. sain and C. B. Schrader, "The role of Zeros in the performance of Multiinput, Multioutput feedback systems", IEEE Transaction on Education, Vol. 33-3, pp. 244-257, 1990.
- [16] P. Kundur, "Power System Stability and Control", New York: McGraw-Hill, 1994
- [17] T. C. Yang, "Applying H_{∞} optimization method to power system stabilizer design part1: single-machine infinite-bus systems", Electrical Power & Energy Systems, Vol. 19, No.1, pp 29-35, 1997.
- [18] P. M. Anderson, and A. A. Fouad, "Power system control and stability", IEEE press, 1993.

Appendix I

The constants k_1, \dots, k_6 are evaluated with transmission line resistance $r_e=0$ and are given as follows:

$$k_1 = \frac{(x_q - x'_d)}{(x_e + x'_d)} I_{q0} V_0 \sin \delta_0 + \frac{E_{q0} V_0 \cos \delta_0}{(x_e + x_q)}$$

$$k_2 = \frac{V_0 \sin \delta_0}{(x_e + x'_d)}$$

$$k_3 = \frac{(x'_d + x_e)}{(x_d + x_e)}$$

$$k_4 = \frac{(x_d - x'_d)}{(x_e + x'_d)} V_0 \sin \delta_0$$

$$k_5 = \frac{x_q}{(x_e + x_q)} \frac{V_{d0}}{V_{t0}} V_0 \cos \delta_0 + \frac{x'_d}{(x_e + x'_d)} \frac{V_{q0}}{V_{t0}} V_0 \sin \delta_0$$

$$k_6 = \frac{x_e}{(x_e + x'_d)} \frac{V_{q0}}{V_{t0}}$$